Pergamon

Int. J. Solids Structures Vol. 35, No. 18, pp. 2229–2249, 1998

0020–7683/98 $19.00 + .00

PII: S0020–7683(97)00188–1

HYPERSINGULAR BOUNDARY ELEMENT FORMULATION FOR REISSNER PLATES

Y. F. RASHED
Structural Engineering Department, Cairo University, Cairo, Egypt

M. H. ALIABADI†
Department of Engineering, Queen Mary College, University of London, London E1 4NS, UK

C. A. BREBBIA
WIT, Southampton, UK

(*Received* 30 *May* 1996; *in revised form* 14 *June* 1997)

Abstract—In this work, the hypersingular boundary element formulation for plate bending analysis based on Reissner theory is presented. First order Taylor expansion are used to deal with the strong singularity $O(1/r)$, whereas, rigid body considerations together with the Taylor expansion are used to compute the hypersingular kernels $O(1/r^2)$. The plate boundary is discretised into quadratic isoparametric discontinuous boundary elements to satisfy the continuity requirements for the boundary unknowns. Several examples are tested, including thin and thick plates. The results show a good agreement with both the analytical solutions and the corresponding results for the standard displacement boundary element formulation. © 1998 Elsevier Science Ltd. All rights reserved

1. INTRODUCTION

In recent years, the application of the boundary element method (BEM) to plate bending problems has gained some popularity. There are many publications in the literature applying the BEM to the Kirchhoff-Love plate theory (see e.g. Bezine (1978), Stern (1979) and Tottenham (1979)). However, this formulation lacks the sufficient number of boundary conditions and does not account for transverse shear deformations. In addition, it yields inaccurate distribution of the resultant shear force for the case of supported plate edge.

Reissner (1945) and (1947) presented a sixth order partial deferential equation theory, which accounted for both the bending and transverse shear stresses. This theory has become the general theory (Karam and Telles (1988)) in plate bending analysis, and allows analysis of both thin and thick plates. Beams of rectangle cross sections may be analyzed with Reissner's theory as shown in Karam and Telles (1992).

Vinturini and Paiva (1993) pointed out that using thin plate theory decreases the problem dimension and the computational time. Guo-Shu and Mukherjee (1986) demonstrated that by using thin plate theory with an additional degree of freedom for the tangential boundary rotation (which gives the problem same dimensions as that of the Reissner theory) many problems associated with that theory can be overcome. Recently, Paiva and Neto (1995) confirmed the findings reported by Guo-Shu and Mukherjee (1986) when dealing with slab-beam interaction problems. This demonstrates the advantage of the Reissner plate theory over the thin plate theory.

Due to the stability and the wide range of applications of Reissner theory, some researchers have applied the BEM to this theory. One of the early applications is due to Vander Weeën (1982a) and (1982b) who derived the boundary integral equation and successfully applied it to several problems.

† Corresponding author.

Antes (1984a) tested the modified Trefftz method and the regular BEM. However, the latter may not be a reliable method as it is dependent on the number and the location of the collocation nodes. The indirect BEM for simply supported plates was presented by Antes (1986). Other contributions regarding the geometric and stress singularities due to concentrated loads can be found in Antes (1984b) and (1985).

Karam and Telles (1988) confirmed that Reissner's plate model is suitable for both thin and thick plates. They extend the formulation to account for infinite regions. Later, Long, *et al.* (1988), presented several problems of thin plates with sharp corners.

Barcellos and Silva (1989) presented a similar formulation to that of Vander Weeën (1982a) for Mindlin plate model. Their formulation differs from Reissner theory in the shear factor constant. Westphal and Barcellos (1990) discussed the importance of the neglected terms in the fundamental solution derived by Vander Weeën (1982a). They concluded that these terms have no effect on the results. They also showed how to move from the Reissner fundamental solution to the Kirchhoff-Love fundamental solution, by assigning zeros to the kernel parts related to shear deformations (Barcellos and Westphal (1992)).

An alternative BEM formulation was derived by Katsikadelis and Yotis (1993). Their formulation was expressed in terms of two potentials: a biharmonic and Bessel potential. This method also depends on the solution of three integral equations plus three finite difference equations. No free edge boundary conditions was presented in their work.

El-Zafrany *et al.* (1994) derived the same fundamental solution for Reissner plate theory as that of Vander Weeën (1982a), but here based on the Hankel integral transformation. In their work El-Zafrany *et al.* (1995), the transverse shear effect was separated from the fundamental solution kernels to allow the analysis of thin plates (i.e., neglecting the effect of the separated shear kernels). As it will be seen in this work, if accurate integration schemes are used to evaluate the boundary element integrals, Reissner's theory can be used for the analysis of plates of any thickness.

Xiao-Yan (1995) presented a new boundary integral formulation for Reissner's plate theory. The main idea of this formulation, is to define new unknown boundary values in terms of boundary stresses. So that, the boundary stresses can be directly computed in the numerical solution, avoiding the use of both the boundary displacement derivatives and finite difference schemes. It is worth noting that the fundamental solution in (Xiao-Yan (1995)) has the same behaviour and order of singularity as the one by Vander Weeën (1982a). This is because, both of the formulations are based on the same weighted residual statement but different in the consideration of the boundary conditions.

Recently, the application of the hypersingular integral equation has been utilized in elasticity problems and acoustics. These hypersingular integral equations have higher order of singularity than the displacement boundary integral equation. There are many applications of the hypersingular equation in elasticity problems, such as the direct evaluation of the boundary stress tensor (see e.g. Huber *et al.* (1996)), crack modeling using the dual BEM (see e.g. Portela *et al.* (1993)) and error estimation in the boundary element analysis via the hypersingular residuals (see e.g. Paulino *et al.* (1996) and Guiggiani (1996)). However, to the author's knowledge, the general derivation and the use of the hypersingular equation in plate bending analysis via the BEM has not been reported.

In this work, the hypersingular stress boundary integral equations are derived by considering the behaviour of the stress integral identity at a boundary point. The Taylor series method was used to expand the terms inside the singular kernels around the singular point. All of the singular integrals are taken in either the Cauchy principal value sense or the Hadamard finite part sense. First order Taylor expansion was used to deal with strong singularity $O(1/r)$, whereas, rigid body consideration together with the Taylor expansion were used to compute the hypersingular kernels $O(1/r^2)$.

The plate boundary is discretised into discontinuous quadratic boundary elements to satisfy the continuity requirement for the boundary unknowns (Portela *et al.* (1993)). Several examples of plates with different thickness and beams are tested. The results show a good agreement with both of the analytical solutions and the corresponding results of the standard displacement boundary element formulation.

2. BASIC THEORY AND THE FUNDAMENTAL SOLUTIONS

In this section, the basic equations of the Reissner plate bending theory are reviewed. Throughout this paper, the indicial notation is used. Greek indices will vary from 1 to 2 whereas, Roman indices from 1 to 3. The comma subscript will be used to denote differentiation, such as $(\cdot)_{,\alpha}$, stands for the derivative of $(\cdot)$ with respect to the coordinate x_α.

Now, consider an arbitrary plate of thickness h, as shown in Fig. 1 with a domain Ω and boundary Γ in the x_i space. The x_1-x_2 plane is assumed to be located at the middle surface $x_3 = 0$. The generalized displacement are denoted as u_i, where, u_α denotes rotations (ϕ_{x_1} and ϕ_{x_2}) and u_3 denotes the transverse deflection w in x_3 direction. According to Reissner (1945), the generalized stress-displacement relationships can be written as follows,

$$M_{\alpha\beta} = D\frac{1-\nu}{2}\left(u_{\alpha,\beta}+u_{\beta,\alpha}+\frac{2\nu}{1-\nu}u_{\gamma,\gamma}\delta_{\alpha\beta}\right)+\frac{\nu q}{(1-\nu)\lambda^2}\delta_{\alpha\beta}$$

$$Q_\alpha = D\frac{1-\nu}{2}\lambda^2(u_\alpha+u_{3,\alpha}) \tag{1}$$

where $M_{\alpha\beta}$ and Q_α are the bending and shear stresses respectively, and $D = Eh^3/12(1-\nu^2)$ is the plate flexural rigidity, E is Young's modulus, ν is Poisson's ratio, $\lambda = \sqrt{10/h}$ is the shear factor and q is the distributed load per unit area. Throughout this paper q is assumed to be constant.

The Equilibrium equations can be written as follows,

$$M_{\alpha\beta,\beta}-Q_\alpha = 0$$
$$Q_{\alpha,\alpha}+q = 0 \tag{2}$$

The generalized tractions at a boundary point can be defined as

$$p_\alpha = M_{\alpha\beta}n_\beta$$
$$p_3 = Q_\alpha n_\alpha \tag{3}$$

where n_β are the components of the outward normal vector to the plate boundary Γ.

The generalized Navier equations can be formed by substituting eqn (1) into eqn (2) to give

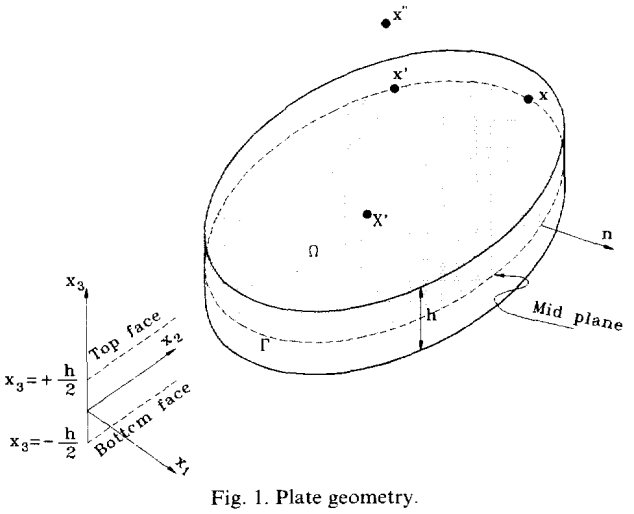

Fig. 1. Plate geometry.

$$L_{ij}^* u_j + b_i = 0 \tag{4}$$

where L_{ij}^* is the generalized Navier differential operator and b_i is the generalized body force components.

The fundamental solution of eqn (4) is obtained by taking $b_{ki} = \delta(\mathbf{X}', \mathbf{X})\delta_{ki}$ where, $\delta(\mathbf{X}', \mathbf{X})$ is the Dirac delta function, k is arbitrary direction of the applied unit load, and $\mathbf{X}$, $\mathbf{X}' \in \Omega$ are the field and source points respectively in an infinite plate.

By using Hörmender method (Vander Weeën (1982a)), the fundamental solution U_{ij}^* can be obtained. Then, the traction fundamental solution P_{ij}^* can be obtained by utilizing eqn (1) together with eqn (3), noting that the differentiation here is with respect to the coordinates of the field point $\mathbf{X}$. The expressions for U_{ij}^* and P_{ij}^* are listed in the Appendix.

It can be seen (from the Appendix) that the fundamental solution is in terms of the following functions

$$A(z) = K_0(z) + \frac{2}{z}\left[K_1(z) - \frac{1}{z}\right]$$

$$B(z) = K_0(z) + \frac{1}{z}\left[K_1(z) - \frac{1}{z}\right] \tag{5}$$

in which $K_0(z)$ and $K_1(z)$ are modified Bessel functions (Abramowitz and Stegun (1965)), $z = \lambda r$ and r is the absolute distance between the source and the field points. By expanding the modified Bessel functions for small arguments (Abramowitz and Stegun (1965)), it can be seen that $A(z)$ is a smooth function, whereas, $B(z)$ is a weekly singular $O(\ln r)$. Therefore U_{ij}^* is a weekly singular and P_{ij}^* has a strong singularity $O(1/r)$.

3. DISPLACEMENT BOUNDARY INTEGRAL EQUATION

The displacement boundary integral equation can be derived from the weighted residual statement (Brebbia *et al.* 1984). Introducing the fundamental fields to this statement, the displacement equation is obtained as:

$$c_{ij}(\mathbf{x}')u_j(\mathbf{x}') + \int_\Gamma P_{ij}^*(\mathbf{x}', \mathbf{x})u_j(\mathbf{x})\,d\Gamma(\mathbf{x}) = \int_\Gamma U_{ij}^*(\mathbf{x}', \mathbf{x})p_j(\mathbf{x})\,d\Gamma(\mathbf{x}) + \int_\Omega \left(U_{i3}^*(\mathbf{x}', \mathbf{X}) - \frac{\nu}{(1-\nu)\lambda^2} U_{i\alpha,\alpha}^*(\mathbf{x}', \mathbf{X})\right) q(\mathbf{X})\,d\Omega(\mathbf{X}) \tag{6}$$

where $\int$ denotes a Cauchy principal value integral, $\mathbf{x}'$, $\mathbf{x} \in \Gamma$ are source point and field point on the boundary respectively, and $c_{ij}(\mathbf{x}')$ are the jump terms from the principal value integral of the strongly singular integral in the kernel P_{ij}^*. The value of $c_{ij}(\mathbf{x}')$ is equal to $1/2\delta_{ij}$ for $\mathbf{x}'$ located on a smooth boundary, however it can be evaluated for a general case from the consideration of the generalized rigid body movements. The domain integral in eqn (6) can be transferred to the boundary integral, in the case of a uniform load (q = constant) to give:

$$\int_\Omega \left(U_{i3}^*(\mathbf{x}', \mathbf{X}) - \frac{\nu}{(1-\nu)\lambda^2} U_{i\alpha,\alpha}^*(\mathbf{x}', \mathbf{X})\right) q(\mathbf{X})\,d\Omega(\mathbf{X}) = q\int_\Gamma \left(V_{i,\alpha}^*(\mathbf{x}', \mathbf{x}) - \frac{\nu}{(1-\nu)\lambda^2} U_{i\alpha}^*(\mathbf{x}', \mathbf{x})\right) n_\alpha(\mathbf{x})\,d\Gamma(\mathbf{x}) \tag{7}$$

where V_i^* are the particular integrals of the equations $\nabla^2 V_i^* = U_{i3}^*$ and the expression for $V_{i,\alpha}^*$ can be found in the Appendix.

Equation (6) represents three integral equations (two ($i = \alpha = 1, 2$) for rotations and one ($i = 3$) for deflection).

Bending and shear stresses at any internal point $\mathbf{X}'$ can be computed by differentiating equation (6) with respect to the coordinate of the source point $\mathbf{X}'$ and then substituting in equation (1) to give

$$M_{\alpha\beta}(\mathbf{X}') = \int_\Gamma U^*_{\alpha\beta k}(\mathbf{X}', \mathbf{x}) p_k(\mathbf{x})\, d\Gamma(\mathbf{x}) - \int_\Gamma P^*_{\alpha\beta k}(\mathbf{X}', \mathbf{x}) u_k(\mathbf{x})\, d\Gamma(\mathbf{x}) + q \int_\Gamma W^*_{\alpha\beta}(\mathbf{X}', \mathbf{x})\, d\Gamma(\mathbf{x}) + \frac{\nu}{(1-\nu)\lambda^2} q\delta_{\alpha\beta}$$

$$Q_\beta(\mathbf{X}') = \int_\Gamma U^*_{3\beta k}(\mathbf{X}', \mathbf{x}) p_k(\mathbf{x})\, d\Gamma(\mathbf{x}) - \int_\Gamma P^*_{3\beta k}(\mathbf{X}', \mathbf{x}) u_k(\mathbf{x})\, d\Gamma(\mathbf{x}) + q \int_\Gamma W^*_{3\beta}(\mathbf{X}', \mathbf{x})\, d\Gamma(\mathbf{x}) \tag{8}$$

where the kernels U^*_{ijk}, P^*_{ijk} and $W^*_{i\beta}$ are given in the Appendix.

As it can be seen the kernels U^*_{ijk} and $W^*_{i\beta}$ contain weak and strong singularities, respectively, whereas, the kernel P^*_{ijk} contains strong and hypersingular terms as $\mathbf{X}' \to \Gamma$.

4. STRESS BOUNDARY INTEGRAL EQUATION

Equation (6) is also valid for an external point $\mathbf{X}'' \notin \Omega, \Gamma$ with $c_{ij} = 0$. The corresponding stress identity may be obtained in similar way as eqn (8) to give

$$\int_\Gamma P^*_{\alpha\beta k}(\mathbf{X}'', \mathbf{x}) u_k(\mathbf{x})\, d\Gamma(\mathbf{x}) = \int_\Gamma U^*_{\alpha\beta k}(\mathbf{X}'', \mathbf{x}) p_k(\mathbf{x})\, d\Gamma(\mathbf{x}) + q \int_\Gamma W^*_{\alpha\beta}(\mathbf{X}'', \mathbf{x})\, d\Gamma(\mathbf{x})$$

$$\int_\Gamma P^*_{3\beta k}(\mathbf{X}'', \mathbf{x}) u_k(\mathbf{x})\, d\Gamma(\mathbf{x}) = \int_\Gamma U^*_{3\beta k}(\mathbf{X}'', \mathbf{x}) p_k(\mathbf{x})\, d\Gamma(\mathbf{x}) + q \int_\Gamma W^*_{3\beta}(\mathbf{X}'', \mathbf{x})\, d\Gamma(\mathbf{x}) \tag{9}$$

The stress boundary integral equation is formed by considering the behaviour of eqn (9) when the point $\mathbf{X}''$ tends to the boundary Γ at $\mathbf{x}'$. To satisfy the continuity requirements, the point $\mathbf{x}'$ is assumed to be on a smooth boundary. A semicircular domain with boundary Γ^*_ε is constructed around the point $\mathbf{x}'$ as shown in Fig. 2.

Taking the limit as $\mathbf{X}'' \to \mathbf{x}'$, eqn (9) can be rewritten as follows

$$\lim_{\varepsilon\to 0} \int_{\Gamma-\Gamma_\varepsilon+\Gamma^*_\varepsilon} P^*_{\alpha\beta\gamma}(\mathbf{x}', \mathbf{x}) u_\gamma(\mathbf{x})\, d\Gamma(\mathbf{x}) + \lim_{\varepsilon\to 0} \int_{\Gamma-\Gamma_\varepsilon+\Gamma^*_\varepsilon} P^*_{\alpha\beta 3}(\mathbf{x}', \mathbf{x}) u_3(\mathbf{x})\, d\Gamma(\mathbf{x})$$
$$= \lim_{\varepsilon\to 0} \int_{\Gamma-\Gamma_\varepsilon+\Gamma^*_\varepsilon} U^*_{\alpha\beta\gamma}(\mathbf{x}', \mathbf{x}) p_\gamma(\mathbf{x})\, d\Gamma(\mathbf{x}) + \lim_{\varepsilon\to 0} \int_{\Gamma-\Gamma_\varepsilon+\Gamma^*_\varepsilon} U^*_{\alpha\beta 3}(\mathbf{x}', \mathbf{x}) p_3(\mathbf{x})\, d\Gamma(\mathbf{x}) + q \lim_{\varepsilon\to 0} \int_{\Gamma-\Gamma_\varepsilon+\Gamma^*_\varepsilon} W^*_{\alpha\beta}(\mathbf{x}', \mathbf{x})\, d\Gamma(\mathbf{x}) \tag{10}$$

and

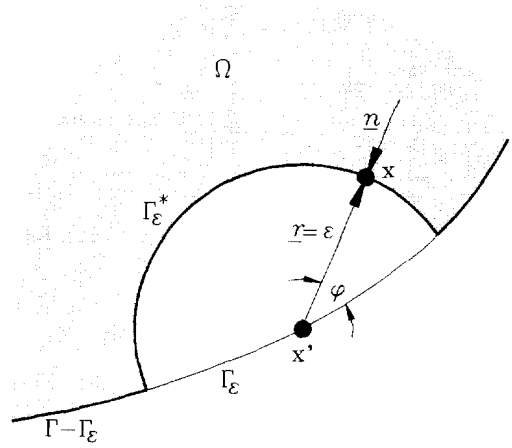

Fig. 2. The semicircular region around the source point.

$$\lim_{\varepsilon\to 0}\int_{\Gamma-\Gamma_\varepsilon+\Gamma_\varepsilon^*} P^*_{3\beta\gamma}(\mathbf{x}',\mathbf{x})u_\gamma(\mathbf{x})\,d\Gamma(\mathbf{x}) + \lim_{\varepsilon\to 0}\int_{\Gamma-\Gamma_\varepsilon+\Gamma_\varepsilon^*} P^*_{3\beta 3}(\mathbf{x}',\mathbf{x})u_3(\mathbf{x})\,d\Gamma(\mathbf{x})$$

$$= \lim_{\varepsilon\to 0}\int_{\Gamma-\Gamma_\varepsilon+\Gamma_\varepsilon^*} U^*_{3\beta\gamma}(\mathbf{x}',\mathbf{x})p_\gamma(\mathbf{x})\,d\Gamma(\mathbf{x}) + \lim_{\varepsilon\to 0}\int_{\Gamma-\Gamma_\varepsilon+\Gamma_\varepsilon^*} U^*_{3\beta 3}(\mathbf{x}',\mathbf{x})p_3(\mathbf{x})\,d\Gamma(\mathbf{x})$$

$$+ q\lim_{\varepsilon\to 0}\int_{\Gamma-\Gamma_\varepsilon+\Gamma_\varepsilon^*} W^*_{3\beta}(\mathbf{x}',\mathbf{x})\,d\Gamma(\mathbf{x}) \qquad (11)$$

Equations (10) and (11) represent the bending stress and shear stress boundary integrals, respectively, at the boundary point $\mathbf{x}'$.

4.1. *The bending stress integral equation*

Equation (10) can be written in the following form

$$I_1^* + I_2^* = I_3^* + I_4^* + I_5^* \qquad (12)$$

Assuming the boundary values of u_i are $C^{1,\alpha}$, $(0 < \alpha < 1)$ and using a Taylor expansion for the integrands up to two terms, the integral I_1^* can be written as

$$I_1^* = \lim_{\varepsilon\to 0}\int_{\Gamma-\Gamma_\varepsilon+\Gamma_\varepsilon^*} P^*_{\alpha\beta\gamma}(\mathbf{x}',\mathbf{x})u_\gamma(\mathbf{x})\,d\Gamma(\mathbf{x}) = \lim_{\varepsilon\to 0}\int_{\Gamma-\Gamma_\varepsilon} P^*_{\alpha\beta\gamma}(\mathbf{x}',\mathbf{x})u_\gamma(\mathbf{x})\,d\Gamma(\mathbf{x})$$

$$+\lim_{\varepsilon\to 0}\int_{\Gamma_\varepsilon^*} P^*_{\alpha\beta\gamma}(\mathbf{x}',\mathbf{x})[u_\gamma(\mathbf{x}) - u_\gamma(\mathbf{x}') - u_{\gamma,\theta}(\mathbf{x}')(\mathbf{x}_\theta - \mathbf{x}'_\theta)]\,d\Gamma(\mathbf{x})$$

$$+u_\gamma(\mathbf{x}')\lim_{\varepsilon\to 0}\int_{\Gamma_\varepsilon^*} P^*_{\alpha\beta\gamma}(\mathbf{x}',\mathbf{x})\,d\Gamma(\mathbf{x}) + u_{\gamma,\theta}(\mathbf{x}')\lim_{\varepsilon\to 0}\int_{\Gamma_\varepsilon^*} P^*_{\alpha\beta\gamma}(\mathbf{x}',\mathbf{x})(\mathbf{x}_\theta - \mathbf{x}'_\theta)\,d\Gamma(\mathbf{x}) \qquad (13)$$

It has to be noted that the integral I_1^* contains the kernel $P^*_{\alpha\beta\gamma}$ which is hypersingular of $O(1/r^2)$ so that two terms of the Taylor expansion for the integrand are appropriate.

In the above integrals, the second term of the right hand side (RHS) is zero in the limit as $\varepsilon \to 0$. The first and third RHS terms together form a Hadamard finite part integral. From Fig. 2, the following relationships can be observed

$$r = \varepsilon, \quad r_{,n} = -1, \quad d\Gamma = \varepsilon\,d\varphi, \quad r_{,1} = -n_1 = \cos\varphi, \quad r_{,2} = -n_2 = \sin\varphi,$$

and

$$\int_{\Gamma_\varepsilon^*} \cdots \mathrm{d}\Gamma_\varepsilon^* = \int_0^\pi \cdots \varepsilon \,\mathrm{d}\varphi \tag{14}$$

By considering the above relationships, together with the following limits (Abramowitz and Stegun (1965))

$$\lim_{\varepsilon\to 0} A(\lambda\varepsilon) = \frac{-1}{2}, \quad \lim_{\varepsilon\to 0} \lambda^2\varepsilon^2 K_0(\lambda\varepsilon) = 0, \quad \lim_{\varepsilon\to 0} \lambda\varepsilon K_1(\lambda\varepsilon) = 1,$$

and

$$\lim_{\varepsilon\to 0} \lambda^2\varepsilon^2 B(\lambda\varepsilon) = 0, \tag{15}$$

the last term on the RHS leads to the following jump terms

$$u_{\gamma,\theta}(\mathbf{x}') \lim_{\varepsilon\to 0} \int_{\Gamma_\varepsilon^*} P^*_{\alpha\beta\gamma}(\mathbf{x}', \mathbf{x})(\mathbf{x}_\theta - \mathbf{x}'_\theta)\,\mathrm{d}\Gamma(\mathbf{x}) = \frac{D(1+\nu)(1-\nu)}{16}(u_{\beta,\alpha}(\mathbf{x}') + u_{\alpha,\beta}(\mathbf{x}') + u_{\gamma,\gamma}(\mathbf{x}')\delta_{\alpha\beta}) \tag{16}$$

Now, the integral I_1^* can be written as follows

$$I_1^* = \oint_\Gamma P^*_{\alpha\beta\gamma}(\mathbf{x}', \mathbf{x}) u_\gamma(\mathbf{x})\,\mathrm{d}\Gamma(\mathbf{x}) + \frac{D(1+\nu)(1-\nu)}{16}(u_{\beta,\alpha}(\mathbf{x}') + u_{\alpha,\beta}(\mathbf{x}') + u_{\gamma,\gamma}(\mathbf{x}')\delta_{\alpha\beta}) \tag{17}$$

where $\oint$ denotes the Hadamard finite part integral.

The integral I_2^* can be treated in a similar way as that of the integral I_1^*. Only one term of Taylor expansion is needed for I_2^* as the kernel $P^*_{\alpha\beta 3}$ contains a strong singularity of $O(1/r)$. So that the integral I_2^* can be written as follows

$$I_2^* = \lim_{\varepsilon\to 0} \int_{\Gamma-\Gamma_\varepsilon+\Gamma_\varepsilon^*} P^*_{\alpha\beta 3}(\mathbf{x}', \mathbf{x}) u_3(\mathbf{x})\,\mathrm{d}\Gamma(\mathbf{x}) = \lim_{\varepsilon\to 0} \int_{\Gamma-\Gamma_\varepsilon} P^*_{\alpha\beta 3}(\mathbf{x}', \mathbf{x}) u_3(\mathbf{x})\,\mathrm{d}\Gamma(\mathbf{x}) + \lim_{\varepsilon\to 0} \int_{\Gamma_\varepsilon^*} P^*_{\alpha\beta 3}(\mathbf{x}', \mathbf{x})[u_3(\mathbf{x}) - u_3(\mathbf{x}')]\,\mathrm{d}\Gamma(\mathbf{x}) + u_3(\mathbf{x}') \lim_{\varepsilon\to 0} \int_{\Gamma_\varepsilon^*} P^*_{\alpha\beta 3}(\mathbf{x}', \mathbf{x})\,\mathrm{d}\Gamma(\mathbf{x}) \tag{18}$$

In the above integrals, the second term on the RHS is zero in the limit as $\varepsilon \to 0$. The first term on the RHS form a Cauchy principal value integral. By considering the relationships in eqn (14) and the limits in eqn (15), the jump terms that appear from the last term on the RHS vanish. So that the integral I_2^* can be written as follows

$$I_2^* = \oint_\Gamma P^*_{\alpha\beta 3}(\mathbf{x}', \mathbf{x}) u_3(\mathbf{x})\,\mathrm{d}\Gamma(\mathbf{x}) \tag{19}$$

In a similar way, the integrals I_3^*, I_4^* and I_5^* can be treated. Noting that the weak singular terms do not lead to any jump terms, the final forms for these integrals can be obtained as follows

$$I_3^* = \int_\Gamma U_{\alpha\beta\gamma}^*(\mathbf{x}',\mathbf{x})p_\gamma(\mathbf{x})\,d\Gamma(\mathbf{x}) - \left(\frac{(3\nu-1)}{16}M_{\gamma\gamma}(\mathbf{x}')\delta_{\alpha\beta} - \frac{2(\nu-3)}{16}M_{\alpha\beta}(\mathbf{x}')\right), \tag{20}$$

$$I_4^* = \int_\Gamma U_{\alpha\beta 3}^*(\mathbf{x}',\mathbf{x})p_3(\mathbf{x})\,d\Gamma(\mathbf{x}), \tag{21}$$

and

$$I_5^* = q\int_\Gamma W_{\alpha\beta}^*(\mathbf{x}',\mathbf{x})\,d\Gamma(\mathbf{x}) + \frac{\nu q}{(1-\nu)\lambda^2}\frac{(1+\nu)}{4}\delta_{\alpha\beta} \tag{22}$$

Now substituting from eqns (17), (19)–(22) into eqn (10), and using eqn (1), it gives

$$\begin{aligned}\frac{1}{2}M_{\alpha\beta}(\mathbf{x}') + \int_\Gamma P_{\alpha\beta\gamma}^*(\mathbf{x}',\mathbf{x})u_\gamma(\mathbf{x})\,d\Gamma(\mathbf{x}) + \int_\Gamma P_{\alpha\beta 3}^*(\mathbf{x}',\mathbf{x})u_3(\mathbf{x})\,d\Gamma(\mathbf{x})\\ = \int_\Gamma U_{\alpha\beta\gamma}^*(\mathbf{x}',\mathbf{x})p_\gamma(\mathbf{x})\,d\Gamma(\mathbf{x}) + \int_\Gamma U_{\alpha\beta 3}^*(\mathbf{x}',\mathbf{x})p_3(\mathbf{x})\Gamma(\mathbf{x})\\ + q\int_\Gamma W_{\alpha\beta}^*(\mathbf{x}',\mathbf{x})\,d\Gamma(\mathbf{x}) + \frac{1}{2}\frac{q\nu}{(1-\nu)\lambda^2}\delta_{\alpha\beta}\end{aligned} \tag{23}$$

which is the bending stress boundary integral equation.

4.2. *The shear stress integral equation*

Equation (11) can be written in the following form

$$I_6^* + I_7^* = I_8^* + I_9^* + I_{10}^* \tag{24}$$

The integrals I_6^* to I_{10}^* can be treated in a similar way as in the treatment of the integrals in the moment stress integral equation, to give

$$I_6^* = \int_\Gamma P_{3\beta\gamma}^*(\mathbf{x}',\mathbf{x})u_\gamma(\mathbf{x})\,d\Gamma(\mathbf{x}) + \frac{D(1-\nu)\lambda^2}{8}u_\beta(\mathbf{x}'), \tag{25}$$

$$I_7^* = \int_\Gamma P_{3\beta 3}^*(\mathbf{x}',\mathbf{x})u_3(\mathbf{x})\,d\Gamma(\mathbf{x}) + \frac{D(1-\nu)\lambda^2}{8}u_{3,\beta}(\mathbf{x}'), \tag{26}$$

$$I_8^* = \int_\Gamma U_{3\beta\gamma}^*(\mathbf{x}',\mathbf{x})p_\gamma(\mathbf{x})\,d\Gamma(\mathbf{x}), \tag{27}$$

$$I_9^* = \int_\Gamma U_{3\beta 3}^*(\mathbf{x}',\mathbf{x})p_3(\mathbf{x})\,d\Gamma(\mathbf{x}) - \frac{Q_\beta(\mathbf{x}')}{4}, \tag{28}$$

and

$$I_{10}^* = q\int_\Gamma W_{3\beta}^*(\mathbf{x}',\mathbf{x})\,d\Gamma(\mathbf{x}) \tag{29}$$

Substituting from eqns (25)–(29) into eqn (11), and using eqn (1) gives

$$\frac{1}{2}Q_\beta(\mathbf{x}')+\int_\Gamma P^*_{3\beta\gamma}(\mathbf{x}',\mathbf{x})u_\gamma(\mathbf{x})\,d\Gamma(\mathbf{x})+\int_\Gamma P^*_{3\beta3}(\mathbf{x}',\mathbf{x})u_3(\mathbf{x})\,d\Gamma(\mathbf{x})$$
$$=\int_\Gamma U^*_{3\beta\gamma}(\mathbf{x}',\mathbf{x})p_\gamma(\mathbf{x})\,d\Gamma(\mathbf{x})+\int_\Gamma U^*_{3\beta3}(\mathbf{x}',\mathbf{x})p_3(\mathbf{x})\,d\Gamma(\mathbf{x})+q\int_\Gamma W^*_{3\beta}(\mathbf{x}',\mathbf{x})\,d\Gamma(\mathbf{x}) \quad (30)$$

which is the shear stress boundary integral equation.

Equations (23) and (30) represent three stress integral equations at a boundary point $\mathbf{x}'$. These equations can be used in a post-processing procedure to evaluate the stress tensor on the boundary.

If equations (23) and (30) are dotted by n_β at the collocation point $\mathbf{x}'$, the following two expressions can be written

$$\frac{1}{2}p_\alpha(\mathbf{x}')+n_\beta(\mathbf{x}')\int_\Gamma P^*_{\alpha\beta\gamma}(\mathbf{x}',\mathbf{x})u_\gamma(\mathbf{x})\,d\Gamma(\mathbf{x})+n_\beta(\mathbf{x}')\int_\Gamma P^*_{\alpha\beta3}(\mathbf{x}',\mathbf{x})u_3(\mathbf{x})\,d\Gamma(\mathbf{x})$$
$$=n_\beta(\mathbf{x}')\int_\Gamma U^*_{\alpha\beta\gamma}(\mathbf{x}',\mathbf{x})p_\gamma(\mathbf{x})\,d\Gamma(\mathbf{x})+n_\beta(\mathbf{x}')\int_\Gamma U^*_{\alpha\beta3}(\mathbf{x}',\mathbf{x})p_3(\mathbf{x})\,d\Gamma(\mathbf{x})$$
$$+qn_\beta(\mathbf{x}')\int_\Gamma W^*_{\alpha\beta}(\mathbf{x}',\mathbf{x})\,d\Gamma(\mathbf{x})+\frac{1}{2}\frac{qv}{(1-v)\lambda^2}n_\alpha(\mathbf{x}') \quad (31)$$

and

$$\frac{1}{2}p_3(\mathbf{x}')+n_\beta(\mathbf{x}')\int_\Gamma P^*_{3\beta\gamma}(\mathbf{x}',\mathbf{x})u_\gamma(\mathbf{x})\,d\Gamma(\mathbf{x})+n_\beta(\mathbf{x}')\int_\Gamma P^*_{3\beta3}(\mathbf{x}',\mathbf{x})u_3(\mathbf{x})\,d\Gamma(\mathbf{x})$$
$$=n_\beta(\mathbf{x}')\int_\Gamma U^*_{3\beta\gamma}(\mathbf{x}',\mathbf{x})p_\gamma(\mathbf{x})\,d\Gamma(\mathbf{x})+n_\beta(\mathbf{x}')\int_\Gamma U^*_{3\beta3}(\mathbf{x}',\mathbf{x})p_3(\mathbf{x})\,d\Gamma(\mathbf{x})$$
$$+qn_\beta(\mathbf{x}')\int_\Gamma W^*_{3\beta}(\mathbf{x}',\mathbf{x})\,d\Gamma(\mathbf{x}) \quad (32)$$

Equation (31) and (32) represent three integral equations (the hypersingular equations) in terms of boundary tractions, and can either replace or work together with the three displacement integral equations in eqn (6) to form the dual boundary integral formulation.

5. NUMERICAL IMPLEMENTATION

In the present work, quadratic isoparametric elements have been used to discretize the boundary of the plate. The local position of the element nodes are general, to allow for the use of continuous or discontinuous elements. Either the displacement or the traction boundary integral equations can be used. In case of using the traction boundary integral equations, only discontinuous elements are employed, to satisfy the assumed continuity requirements for the boundary variables.

After this discretisation, eqn (6) or eqns (31) and (32) can be written in the following form

$$[H]\{u\}=[G]\{p\}+\{Q\} \quad (33)$$

where $[H]$ and $[G]$ are the well-known boundary element influence matrices, $\{u\}$ and $\{p\}$ are the boundary displacement and traction vectors, respectively, and $\{Q\}$ is the domain load vector. This system of algebraic equations can be solved for the boundary unknowns.

6. SINGULARITIES

In this section, the treatment of the singularities that occur in both of the displacement and the traction boundary integral equations will be discussed. Singularities in the displacement BIE will be reviewed in a quick manner, as it can be found in other references, whereas singularities in the traction BIE will be discussed in detail.

6.1. *Singularities in the displacement BIE*

In the displacement boundary integral equation, the influence $[G]$ matrix and the load vector $\{Q\}$ contain weakly singular kernels, which can be cancelled using a nonlinear coordinate transformation as in Telles (1987). The influence matrix $[H]$, on the other hand, contains a strongly singular kernel, which can be evaluated indirectly using the so called generalized rigid body movements. This can be achieved as follows. If a traction-free problem is considered, three independent cases may be considered:

- $u_1 = C$ then $u_2 = 0$ and $u_3 = -r_1 C$
- $u_2 = C$ then $u_1 = 0$ and $u_3 = -r_2 C$
- $u_3 = C$ then $u_2 = 0$ and $u_2 = 0$

where C is an arbitrary constant and $r_\alpha = \mathbf{x}_\alpha - \mathbf{x}'_\alpha$.

By applying these cases to the system of eqn (33), the following expressions can be written

$$H^{i\alpha}(\mathbf{x}') = -\int_\Gamma [P^*_{i\alpha}(\mathbf{x}', \mathbf{x}) + (-r_\alpha) P^*_{i3}(\mathbf{x}', \mathbf{x})]\, d\Gamma(\mathbf{x})$$

$$H^{i3}(\mathbf{x}') = -\int_\Gamma P^*_{i3}(\mathbf{x}', \mathbf{x})\, d\Gamma(\mathbf{x}) \tag{34}$$

where $H^{ij}(\mathbf{x}')$ (i.e., $H^{i\alpha}(\mathbf{x}')$ and $H^{i3}(\mathbf{x}')$) includes the diagonal sub-matrix and the jump term c_{ij} in the influence matrix $[H]$. The first term in the first integral and the second integral were already computed, however, the second term in the first integral remains to be computed. Fortunately, in this term, the distance r_α cancels the weak singularity in $P^*_{\alpha 3}$ and the strong singularity in P^*_{33} in the singular element under consideration.

6.2. *Singularities in the traction BIE*

In the traction BIE, the singularity order is higher than in the displacement BIE. In this section, each element of eqn (33) will be individually discussed. Three orders of singularity will appear in this formulation. The weak singularity is treated using a nonlinear coordinate transformation as in Telles (1987). The strong singularity is treated using a first order Taylor expansion of the fundamental solution terms around the singular point, as in Aliabadi *et al.* (1985). In this case, the singular term is isolated and integrated analytically. The hypersingular kernels will be computed indirectly using generalized rigid body movements together with the first order Taylor expansion.

The influence matrix [H]. In the $[H]$ matrix, the kernels $P^*_{\alpha\beta 3}$ and $P^*_{3\beta\gamma}$ are strongly singular, whereas, the kernels $P^*_{\alpha\beta\gamma}$ and $P^*_{3\beta 3}$ are hypersingular.

In the off-diagonal sub-matrices (see Fig. 3), the element shape function, will reduce the order of singularities by one. This means that, the elements corresponding to the kernels $P^*_{\alpha\beta 3}$ and $P^*_{3\beta\gamma}$ have smooth integrands, whereas, the elements of the kernels $P^*_{\alpha\beta\gamma}$ and $P^*_{3\beta 3}$ still remain strongly singular.

Now, consider the kernels $P^*_{\alpha\beta\gamma}$ for any off-diagonal sub-matrix, the corresponding integral can be written in the local coordinate system as

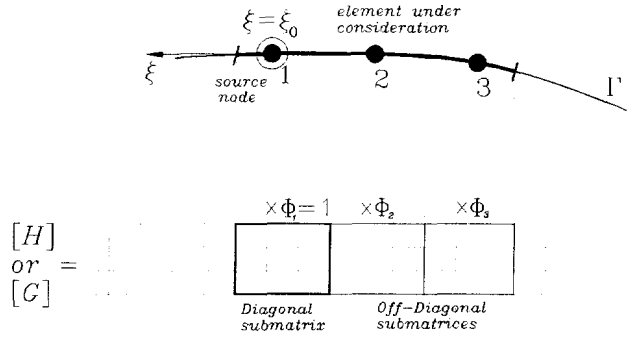

Fig. 3. Sub-matrices for the influence matrices.

$$\int_{\Gamma_e} P^*_{x\beta\gamma}\Phi^i \,d\Gamma = \int_{-1}^{+1} P^*_{x\beta\gamma}\Phi^i(\xi)J(\xi)\,d\xi \tag{35}$$

where Γ_e denotes the boundary of the singular element, Φ^i is the element shape function corresponding to the node i in the element under consideration and J is the Jacobian of the transformation form x_α coordinate system to the local coordinate system ξ (i.e. $d\Gamma = J(\xi)\,d\xi$). To deal with this strong singularity, consider the first order Taylor expansion about the singular point ξ_0 in the local coordinate system, as follows

$$\begin{aligned}
\Phi^i(\xi) &= \Phi^i(\xi_0)+\Phi^{i\prime}(\xi_0)\delta\xi+\frac{1}{2}\Phi^{i\prime\prime}(\xi_0)\delta\xi^2+\ldots\\
J(\xi) &= J(\xi_0)+J'(\xi_0)\delta\xi+\frac{1}{2}J''(\xi_0)\delta\xi^2+\ldots\\
x_\alpha(\xi) &= x_\alpha(\xi_0)+x'_\alpha(\xi_0)\delta\xi+\frac{1}{2}x''_\alpha(\xi_0)\delta\xi^2+\ldots
\end{aligned} \tag{36}$$

in which

$$x_\alpha(\xi) = \sum_{i=1}^{3} M^i(\xi)x^i_\alpha \tag{37}$$

where, x^i_α is the coordinate x_α at the nodal point i, M^i are the geometric shape functions, $(\,\cdot\,)'$ denotes the derivatives of $(\,\cdot\,)$ with respect to ξ and $\delta\xi = \xi-\xi_0$. Using eqn (36), the following expressions for the quadratic element can be written (Aliabadi *et al.* (1985))

$$\begin{aligned}
r_\alpha &= x'_\alpha(\xi_0)\delta\xi+\frac{1}{2}x''_\alpha(\xi_0)\delta\xi^2\\
r &= |\delta\xi|\sqrt{d_0+d_1\delta\xi+d_2\delta\xi^2}
\end{aligned} \tag{38}$$

where

$$\begin{aligned}
d_0 &= x'_\alpha(\xi_0)x'_\alpha(\xi_0)\\
d_1 &= x'_\alpha(\xi_0)x''_\alpha(\xi_0)\\
d_2 &= \frac{1}{4}x''_\alpha(\xi_0)x''_\alpha(\xi_0)
\end{aligned} \tag{39}$$

Noting that in the case of the off-diagonal sub-matrices $\Phi^i(\xi^{\text{node}}) = 0$ for $\xi^{\text{node}} \neq \xi_0$,

and using the expressions in eqns (36) and (38), together with the limits in eqn (15), eqn (35) can be written in the following form

$$\int_{-1}^{+1} P^*_{\alpha\beta\gamma}\,\Phi^i(\xi)J(\xi)\,d\xi = \int_{-1}^{+1} [P^*_{\alpha\beta\gamma}\,\Phi^i(\xi)J(\xi) - S^H_{\alpha\beta\gamma}(\xi_0)]\,d\xi + \int_{-1}^{+1} S^H_{\alpha\beta\gamma}(\xi_0)\,d\xi \tag{40}$$

and

$$S^H_{\alpha\beta\gamma}(\xi_0) = \frac{D(1-\nu)}{4\pi}\Phi^{i'}J\{[(1-\nu)(\delta_{\gamma\alpha}n_\beta + \delta_{\gamma\beta}n_\alpha) + (-1+3\nu)\delta_{\alpha\beta}n_\gamma]\mathscr{T}_1$$
$$+[-2(1-\nu)(n_\alpha x'_\beta x'_\gamma + n_\beta x'_\alpha x'_\gamma + \delta_{\gamma\alpha}x'_\beta x'_\theta n_\theta + \delta_{\gamma\beta}x'_\alpha x'_\theta n_\theta) - 2(\nu-1)(\delta_{\alpha\beta}x'_\gamma x'_\theta n_\theta + n_\gamma x'_\alpha x'_\beta)]\mathscr{T}_2$$
$$-[8(1+\nu)(x'_\alpha x'_\beta x'_\gamma x'_\theta n_\theta)]\mathscr{T}_3\} \tag{41}$$

where $S^H_{\alpha\beta\gamma}$ is the isolated singular term, in which all of the involved functions are computed at the singular point ξ_0. The terms $\mathscr{T}_i$ can be defined as follows

$$\mathscr{T}_i = \frac{1}{\delta\xi(d_0 + d_1\delta\xi + d_2\delta\xi^2)^i} \quad i = 1,2,3 \tag{42}$$

As can be seen, the first integral on the RHS of eqn (40) is not singular and can be evaluated using Gauss–Legendre scheme. The second integral is computed in the Cauchy principal value sense and is computed analytically.

Following a similar procedure for $P^*_{3\beta3}$, gives

$$\int_{\Gamma_e} P^*_{3\beta3}\,\Phi^i\,d\Gamma = \int_{-1}^{+1} [P^*_{3\beta3}\Phi^i(\xi)J(\xi) - S^H_{3\beta3}(\xi_0)]\,d\xi + \int_{-1}^{+1} S^H_{3\beta3}(\xi_0)\,d\xi \tag{43}$$

and

$$S^H_{3\beta3}(\xi_0) = \frac{D(1-\nu)\lambda^2}{4\pi}\Phi^{i'}J[n_\beta\mathscr{T}_1 - 2x'_\beta x'_\theta n_\theta\mathscr{T}_2] \tag{44}$$

On the other hand, the diagonal sub-matrices contain strongly singular and hypersingular terms. Herein, the generalized rigid body movements will be considered in a similar way to that of the displacement BIE, to compute these terms indirectly. By considering the generalized rigid body movements, a similar equation to that in eqn (34) is obtained, i.e.,

$$H^{i\alpha}(\mathbf{x}') = -n_\beta(\mathbf{x}')\int_\Gamma [P^*_{i\beta\alpha}(\mathbf{x}',\mathbf{x}) + (-r_\alpha)P^*_{i\beta3}(\mathbf{x}',\mathbf{x})]\,d\Gamma(\mathbf{x})$$
$$H^{i3}(\mathbf{x}') = -n_\beta(\mathbf{x}')\int_\Gamma P^*_{i\beta3}(\mathbf{x}',\mathbf{x})\,d\Gamma(\mathbf{x}) \tag{45}$$

Unlike the displacement BIE, the second term in the first integral of eqn (45) is still singular. The distance r_α cancels the strong singularity in the kernel $P^*_{\alpha\beta3}$; but it only reduces the singularity order of the kernel $P^*_{3\beta3}$ to that of a strong singular kernel. This term is considered in Cauchy principal value sense. By employing a first order Taylor expansion as in eqn (36) together with the limits in eqn (15) for the variables in the integral, and noting that on the diagonal sub-matrices $\Phi^i(\xi^{\text{node}}) = 1$ for $\xi^{\text{node}} = \xi_0$, the following expression can be written

$$\int_{\Gamma_e} (-r_\alpha) P^*_{3\beta 3} \Phi^i \, d\Gamma = \int_{-1}^{+1} [(-r_\alpha) P^*_{3\beta 3} \Phi^i(\xi) J(\xi) - S^{RB}_{\alpha\beta}(\xi_0)] \, d\xi + \int_{-1}^{+1} S^{RB}_{\alpha\beta}(\xi_0) \, d\xi \quad (46)$$

and

$$S^{RB}_{\alpha\beta}(\xi_0) = \frac{-D(1-\nu)\lambda^2}{4\pi} J\{n_\beta x'_\alpha \mathscr{T}_1 - 2x'_\beta x'_\alpha x'_\theta n_\theta \mathscr{T}_2\} \quad (47)$$

where the first integral on the RHS of eqn (46) is not singular, and the second integral contains the singular term and is computed analytically.

The influence matrix [G]. In this matrix, the integrands in the off-diagonal sub-matrices are smooth due to the element shape functions. The diagonal matrices, on the other hand, contain the kernels $U^*_{\alpha\beta 3}$ and $U^*_{3\beta\gamma}$ which are weakly singular. A nonlinear coordinate transformation (Telles, 1987) is used to cancel these singularities. On the other hand, the two kernels, $U^*_{\alpha\beta\gamma}$ and $U^*_{3\beta 3}$ are strongly singular. By employing a first order Taylor expansion (eqn (36)) together with the limits in eqn (15) for the variables in these integrals, and noting that on the diagonal sub-matrices $\Phi^i(\xi^{node}) = 1$ for $\xi^{node} = \xi_0$ the following expressions can be written

$$\int_{\Gamma_e} U^*_{\alpha\beta\gamma} \Phi^i \, d\Gamma = \int_{-1}^{+1} [U^*_{\alpha\beta\gamma} \Phi^i(\xi) J(\xi) - S^G_{\alpha\beta\gamma}(\xi_0)] \, d\xi + \int_{-1}^{+1} S^G_{\alpha\beta\gamma}(\xi_0) \, d\xi \quad (48)$$

$$\int_{\Gamma_e} U^*_{3\beta 3} \Phi^i \, d\Gamma = \int_{-1}^{+1} [U^*_{3\beta 3} \Phi^i(\xi) J(\xi) - S^G_{3\beta 3}(\xi_0)] \, d\xi + \int_{-1}^{+1} S^G_{3\beta 3}(\xi_0) \, d\xi \quad (49)$$

and

$$S^G_{\alpha\beta\gamma}(\xi_0) = \frac{1}{4\pi} J\{[(1-\nu)(\delta_{\beta\gamma} x'_\alpha + \delta_{\alpha\gamma} x'_\beta) + (\nu-1)\delta_{\alpha\beta} x'_\gamma] \mathscr{T}_1 + [2(1+\nu) x'_\alpha x'_\beta x'_\gamma] \mathscr{T}_2\} \quad (50)$$

$$S^G_{3\beta 3}(\xi_0) = \frac{1}{2\pi} J x'_\beta \mathscr{T}_1 \quad (51)$$

where the first integral on the RHS of eqn (48) and eqn (49) is not singular, and the second integral contains the singular term and is computed analytically. The terms $\mathscr{T}_i$ are defined in eqn (42).

The domain load vector {Q}. There are two kernels in the consideration of the domain load vector term. The first kernel is $W^*_{3\beta}$ which is weakly singular, hence, a nonlinear coordinate transformation may be used to treat this kernel. The second one is $W^*_{\alpha\beta}$, which is strongly singular. By employing a first order Taylor expansion (eqns (36) and (38)) together with the limits in eqn (15) for the variables in this integral, the singular term is isolated as follows

$$\int_{\Gamma_e} W^*_{\alpha\beta} \Phi^i \, d\Gamma = \int_{-1}^{+1} [W^*_{\alpha\beta} \Phi^i(\xi) J(\xi) - S^Q_{\alpha\beta}(\xi_0)] \, d\xi + \int_{-1}^{+1} S^Q_{\alpha\beta}(\xi_0) \, d\xi \quad (52)$$

and

$$S^{Q}_{\alpha\beta}(\xi_0) = \frac{-v}{(1-v)\lambda^2}\frac{1}{4\pi}J\{[(1-v)(x'_\alpha n_\beta + x'_\beta n_\alpha) + (v-1)\delta_{\alpha\beta}x'_\gamma n_\gamma]\mathscr{T}_1 + [2(1+v)x'_\alpha x'_\beta x'_\gamma n_\gamma]\mathscr{T}_2\} \quad (53)$$

where the first integral on the RHS of eqn (52) is not singular, and the second integral contains the singular term and is computed analytically. The terms $\mathscr{T}_i$ are defined in eqn (42).

7. NUMERICAL EXAMPLES

In this section, several numerical examples are analyzed using the present boundary element formulation. In all examples quadratic discontinuous boundary elements are used for both the traction boundary integral equation (TBIE) and the displacement boundary integral equation (DBIE) to allow the comparison with the same discretisation scheme; unless stated. The collocation points are placed at $\xi = 0.7, 0, -0.7$. It was found that the numerical results are not significantly affected by the use of continuous or discontinuous elements for the DBIE, or even by the location of the collocation points in the discontinuous elements for both the DBIE or the TBIE. Gauss–Legendre scheme is used to compute the regular integrals with 10 points. The results obtained by the TBIE are compared with analytical solutions and the results from the standard DBIE.

7.1. *Circular clamped thick plate*

In this example, a clamped circular plate is considered. A uniform load of intensity q is applied over the plate domain. Due to symmetry, only one quarter of the plate is modelled. The plate is of radius a and with a thickness of $0.2\,a$. The exact solution for this problem is given in (Vander Weeën (1982a)). Table 1 shows the results obtained together with the exact results. In the case of TBIE the plate was discretized into 16 boundary elements. As can be seen in Table 1 the results are in a good agreement with the exact solutions.

7.2. *Simply supported thin square plate*

Consider a plate shown in Fig. 4. This plate is a square with sides of 4 m length and simply supported from all sides. A uniform load of $-0.64\ tf/m^2$ is applied over the plate domain. Seven internal points are considered (see Fig. 4). Due to the problem symmetry, only one quarter of the plate was modelled in the analysis for the points 1 to 6. The results for point 7 which is located at the center of the plate were obtained by modelling the complete plate. Tables 2, 3 and 4 present the displacements, bending moments and shear stresses at the internal points shown in Fig. 4. The exact results for this problem can be found in (Timoshenko and Woinowsky-Krieger, 1959) and the corresponding numerical results for both the DBIE and the TBIE are based on a model with 64 boundary elements. Referring to (Karam and Telles, 1988), accurate results for the DBIE can be achieved using only eight continuous elements; but it was found that by employing 32 elements the results for the TBIE has an error of 2 to 7%; whereas, with 64 elements (as shown in the tables) the error is within 0.6%.

Table 1. Circular clamped plate results

$\frac{r}{a}$	$\frac{64D}{qa^4}w$		$\frac{16D}{qa^3}\phi_r$		$\frac{16}{qa^2}M_{00}$		$\frac{16}{qa^2}M_{rr}$		$\frac{2}{qa}Q_r$	
	Exact	TBIE	Exact	TBIE	Exact	TBIE	Exact	TBIE	Exact	TBIE
0.00	1.1829	1.1839	0.0000	0.0000	1.3274	1.3329	1.3274	1.3329	0.00	0.00
0.25	1.0503	1.0501	0.2344	0.2342	1.2087	1.2085	1.1212	1.1210	−0.25	−0.25
0.50	0.6996	0.6995	0.3750	0.3750	0.8524	0.8523	0.5024	0.5023	−0.50	−0.50
0.75	0.2714	0.2714	0.3281	0.3281	0.2587	0.2586	−0.5288	−0.5289	−0.75	−0.75
1.00	0.0000	0.0000	0.0000	0.0000	−0.5726	−0.5629	−1.9726	−1.9694	−1.00	−1.00

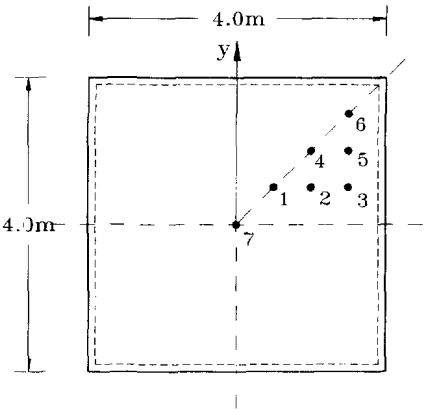

Fig. 4. Simply supported thin square plate.

Table 2. Thin square plate, displacements at internal points

	$\phi_x \times 10^2$ (rad)			$\phi_y \times 10^2$ (rad)			$w \times 10^2$ (m)		
Pt	Exact	DBIE	TBIE	Exact	DBIE	TBIE	Exact	DBIE	TBIE
1	−0.1844	−0.1844	−0.1855	−0.1844	−0.1844	−0.1854	−0.6134	−0.6145	−0.6176
2	−0.3552	−0.3551	−0.3564	−0.1424	−0.1423	−0.1433	−0.4776	−0.4785	−0.4809
3	−0.4902	−0.4902	−0.4916	−0.0778	−0.0778	−0.0785	−0.2641	−0.2645	−0.2664
4	−0.2752	−0.2752	−0.2763	−0.2752	−0.2752	−0.2763	−0.3725	−0.3733	−0.3752
5	−0.3822	−0.3821	−0.3833	−0.1510	−0.1510	−0.1518	−0.2066	−0.2070	−0.2084
6	−0.2117	−0.2116	−0.2125	−0.2117	−0.2116	−0.2125	−0.1151	−0.1154	−0.1163
7	0.0000	0.0000	0.0000	0.0000	0.0000	0.0000	−0.7094	−0.7110	−0.7119

Table 3. Thin square plate, bending moments at internal points

	$M_{xx}(tf \cdot m/m)$			$M_{xy}(tf \cdot m/m)$			$M_{yy}(tf \cdot m/m)$		
Pt	Exact	DBIE	TBIE	Exact	DBIE	TBIE	Exact	DBIE	TBIE
1	−0.4396	−0.4396	−0.4402	0.0378	0.0377	0.0378	−0.4396	−0.4396	−0.4402
2	−0.3744	−0.3745	−0.3749	0.0715	0.0715	0.0717	−0.3504	−0.3505	−0.3509
3	−0.2410	−0.2410	−0.2414	0.0960	0.0960	0.0964	−0.2027	−0.2028	−0.2030
4	−0.3014	−0.3015	−0.3018	0.1367	0.1367	0.1370	−0.3014	−0.3015	−0.3018
5	−0.1982	−0.1983	−0.1985	0.1857	0.1856	0.1861	−0.1769	−0.1770	−0.1772
6	−0.1212	−0.1212	−0.1213	0.2577	0.2576	0.2580	−0.1212	−0.1212	−0.1213
7	−0.4905	−0.4904	−0.4904	0.0000	0.0000	0.0000	−0.4905	−0.4904	−0.4904

Table 4. Thin square plate, shear stresses at internal points

	$Q_x(tf/m)$			$Q_y(tf/m)$		
Pt	Exact	DBIE	TBIE	Exact	DBIE	TBIE
1	0.1529	0.1527	0.1531	0.1529	0.1527	0.1531
2	0.3278	0.3275	0.3279	0.1200	0.1199	0.1203
3	0.5471	0.5467	0.5474	0.0668	0.0667	0.0671
4	0.2613	0.2610	0.2614	0.2613	0.2610	0.2614
5	0.4505	0.4502	0.4506	0.1485	0.1482	0.1485
6	0.2713	0.2710	0.2713	0.2713	0.2710	0.2713
7	0.0000	0.0000	0.0000	0.0000	0.0000	0.0000

7.3. *Thin cantilever plate*

In order to demonstrate the stability of the proposed model over the thin plate theory, the following example is considered. A thin square cantilever plate of side length a is subjected to a uniform load of intensity q over the plate domain. The Poisson ratio was set

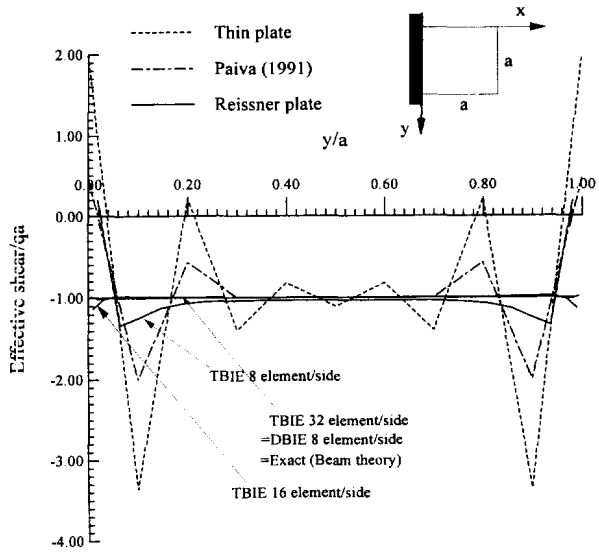

Fig. 5. Shear stresses in the thin cantilever plate.

to zero to allow for the comparison with beam theory. Figure 5 shows the effective shear stress distribution along the clamped edge. As can be seen from Fig. 5, the DBIE gives a stable solution with only a few elements (eight elements per side), whereas, the TBIE gives the same stability with 16 elements per side. The thin plate solution (Paiva, 1991), on the other hand, fails to reach the exact distribution, even with the proposed twisting moment distribution along the boundary according to Paiva (1991).

7.4. *Torsion of cube*

In this example, a three dimensional structure is modelled using the present formulation. Consider a cube of side length of 2 a (as shown in Fig. 6), under torsional rotation at its free end face. To model the loading, the following generalized displacement are prescribed at the free end face,

$$\phi_y = \varphi a$$

$$w = \varphi a y$$

where φ is the applied prescribed torsional rotation.

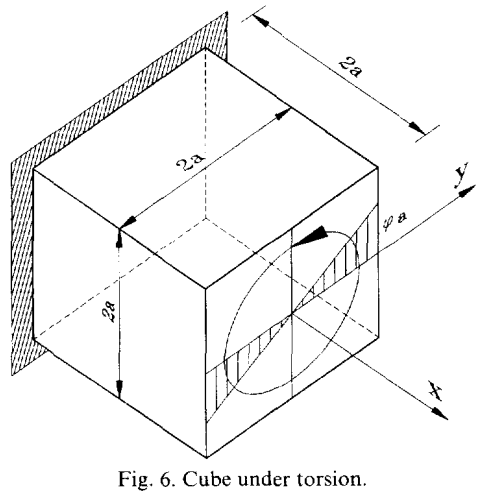

Fig. 6. Cube under torsion.

Table 5. Torsion of cube results

$\frac{y}{a}$	$\frac{\phi_x(y)}{\phi_x(a)}$			$\frac{M_{xz}(y)}{M_{xz}(0)}$			$\frac{Q_x(y)}{Q_x(a)}$		
	Exact	Ref*	TBIE	Exact	Ref*	TBIE	Exact	Ref*	TBIE
0.00	0.000	0.000	0.000	1.000	1.018	1.000	0.000	0.001	0.000
0.25	−0.292	−0.291	−0.290	0.948	0.938	0.948	0.174	0.174	0.174
0.50	−0.387	−0.386	−0.382	0.785	0.809	0.785	0.376	0.377	0.376
0.75	−0.055	−0.053	−0.051	0.485	0.469	0.485	0.638	0.638	0.638
1.00	1.000	1.001	1.000	0.000	0.035	0.000	1.000	0.999	1.000

* Ref: Vander Weeën (1982a).

The problem was analysed using 128 boundary elements to model the high stress concentration and the free edge condition. The results in non-dimensional form are presented in Table 5 together with the results of Vander Weeën (1982a) and the analytical solution given by Reissner (1945). As shown in Table 5, the results of the TBIE are in excellent agreement with the analytical results but they require finer discretisation than the DBIE (Vander Weeën, 1982a).

7.5. *Timoshenko beam*

To demonstrate the capability of the proposed model in analysing beams, a Timoshenko beam of length 10 *m* is considered. The beam has a cross section of 3 *m* depth × 1 *m* width. The following material properties are considered $\nu = 0.2$ and $E = 2 \times 10^6$ t/m^2. The beam was fixed from one end and left free as a cantilever. A concentrated load of $P = 1$ ton is applied at the free end of the beam. A mesh of 20 elements along the beam length (for each side) × 4 elements along the beam width (per side) is used to model the beam mid-plane. The analytical solution for that problem considering shear deformation can be found in Timoshenko and Goodier (1934). The results for the rotation in the x direction and the transverse deflection along the beam center line are plotted together with the analytical results in Fig. 7. The bending moment and shearing force diagrams along the same line are also plotted in Fig. 8. As can be seen from these figures the results of the TBIE are in good agreement with that of the DBIE. A difference (6%) between the BIE and the analytical solution for the maximum deflection of the beam is obtained. It has to be noted that there are small inaccuracies in the bending moment and the shearing force near the fixed edge. These are mainly due to the poor discretisation of the beam width.

7.6. *Stresses on the boundary*

The direct evaluation of stresses on the boundary is one of the important applications of the hypersingular integral equations. To demonstrate this application, the problem of

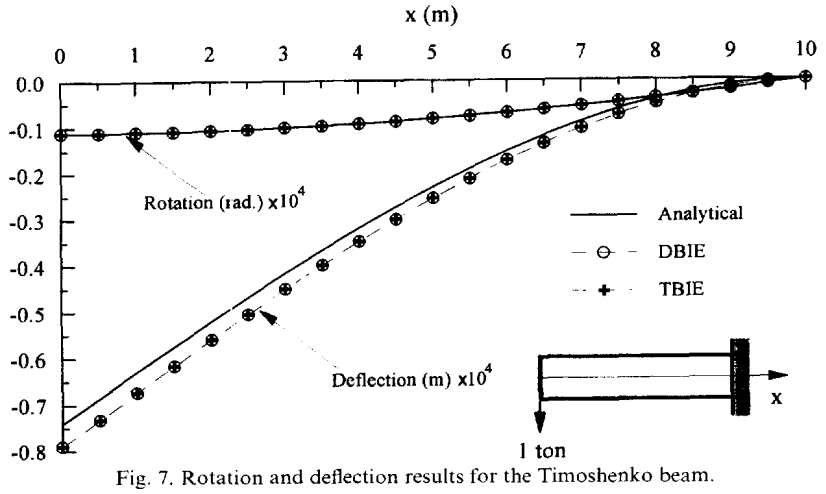

Fig. 7. Rotation and deflection results for the Timoshenko beam.

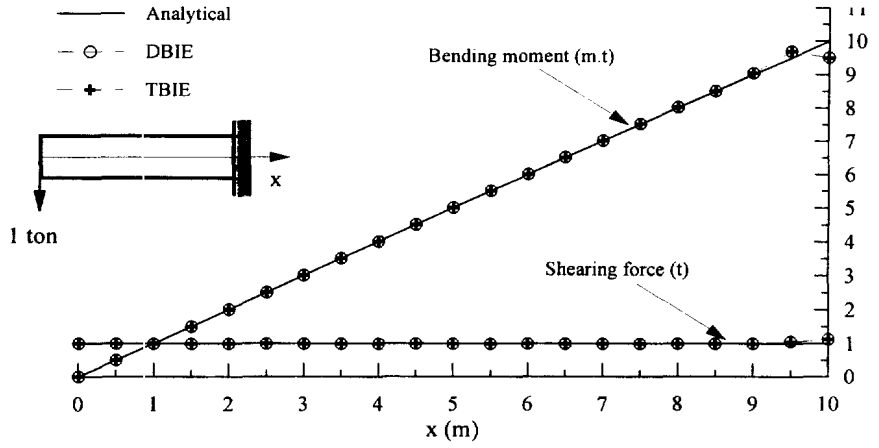

Fig. 8. Bending moment and shearing force results for the Timoshenko beam.

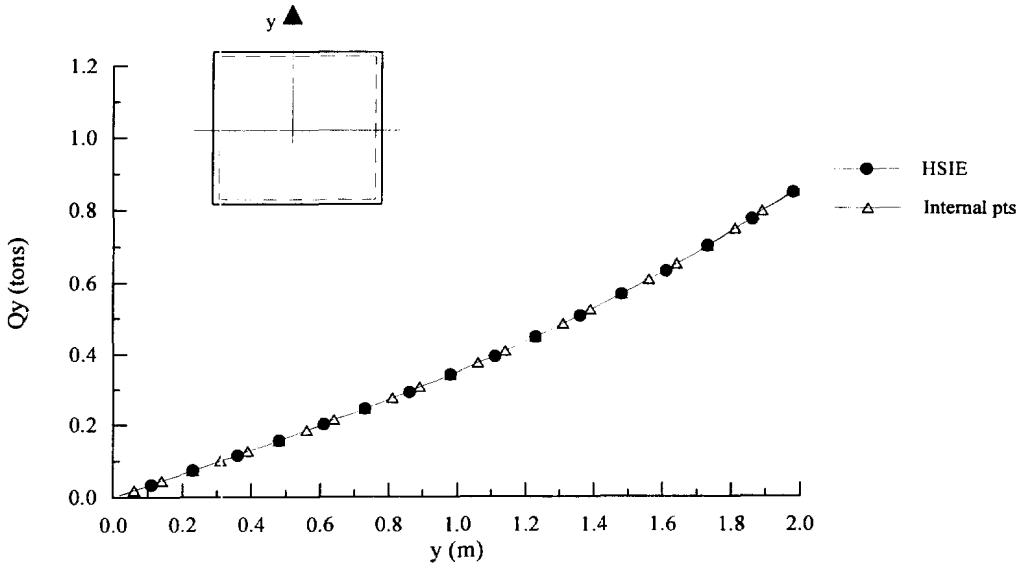

Fig. 9. Shear stress along y-axis for the simply supported plate.

the simply supported plate in example 2 with the same geometry and under the same loading conditions, is considered. The plate was analyzed twice to compare the stresses on a boundary line (y-axes) for a quarter of the plate with the stresses when this line is considered as an internal line for the full plate analysis. In the first analysis, a quarter of the plate was considered by employing 16 boundary elements per side. The stresses were computed directly by employing the hypersingular integral equation (HSIE) in eqns (23) and (30) on the boundary along y-axis, see Fig. 4. In the second analysis, the complete plate was reanalyzed by using 16 continuous boundary elements per side. The stresses were computed at the internal points, which are in the same place as the boundary points in the first analysis. Figures 9 and 10 show the shear stresses and the bending stresses respectively, along the considered line. It can be seen, the results of the hypersingular integral equation are in excellent agreement with the internal point computation of the stresses.

8. CONCLUSIONS

A hypersingular boundary element formulation for plate bending analysis is developed in this work. The formulation utilizes Reissner plate bending theory, which accounts for the transverse shear deformation, and provides an adequate number of the necessary boundary conditions. The formulation was developed by considering the stress identity at a boundary point. By using Taylor series, and assuming an appropriate continuity of the

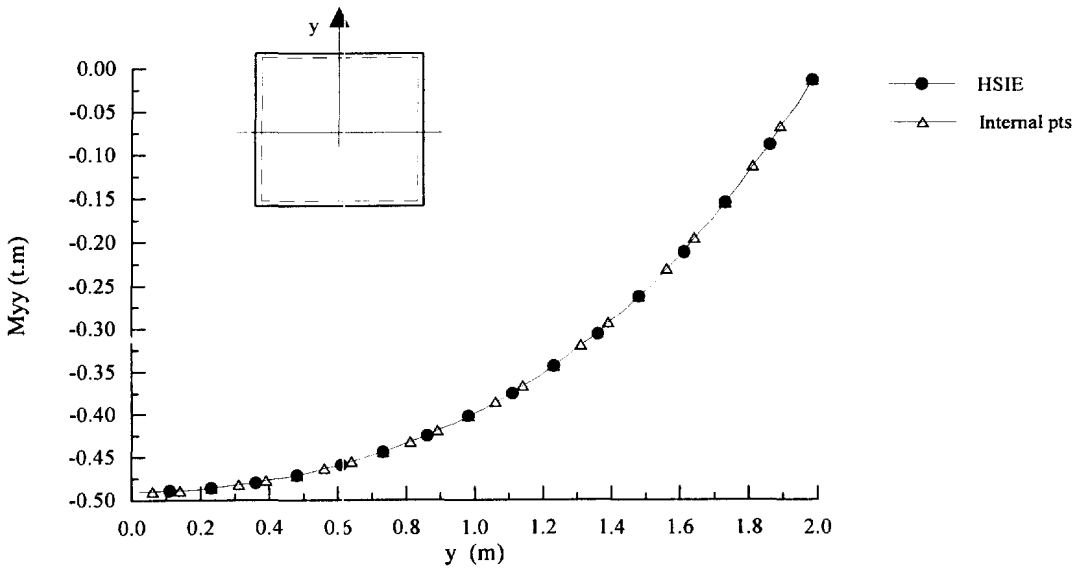

Fig. 10. Bending stress along y-axis for the simply supported plate.

boundary functions, it was shown that the stress integral equations have the same jump term as that of elasticity problems. First order Taylor expansion and rigid body generalized movements were used to compute the singular integrals. Only discontinuous boundary elements were used for the TBIE. Several examples were presented including thick plates, thin plates, and beams. It was shown that considering shear deformations is very important in the stability of the shear resultant tractions. More elements, especially for free edge conditions are required for the TBIE. The presented results are in good agreements with the analytical solutions and those obtained from the standard displacement boundary element formulation. The stress integral equation allows the direct computation of the boundary stresses. This model can be considered as the bases for the dual boundary element formulation.

Acknowledgements—The authors would like to thank the reviewers for their constructive comments on the paper.

REFERENCES

Abramowitz, M. and Stegun, I. A. eds. (1965) *Handbook of Mathematical Functions*. Dover, New York.

Aliabadi, M. H., Hall, W. S. and Phemister, T. G. (1985) Taylor expansion for singular kernels in the boundary element method. *International Journal of Numerical Methods in Engineering* **21**, 2221–2236.

Antes, H. (1984a) On a regular boundary integral equation and a modified Trefftz method in Reissner's plate theory. *Engineering Analysis* **1**, 149–153.

Antes, H. (1984b) The stress functions of point loading in Reissner's plate theory. *Mechanical Research Communications* **11**, 115–120.

Antes, H. (1985) Basic geometrical singularities in Reissner's plate theory. *Mechanical Research Communications* **12**, 295–302.

Antes, H. (1986) An indirectly derived integral equations system for simply supported Reissner plates. *Mechanical Research Communications* **13**, 63–59.

Barcellos, C. A. and Silva, L. H. M. (1989) A boundary element formulation for the Mindlin's plate model. In *BETECH89* (Edited by C. A. Brebbia and W. S. Venturini), pp. 123–130. CMP, Billerica, MA.

Barcellos, C. A. and Westphal, T. Jr. (1992) Reissner/Mindlin's plate models and the boundary element method. In *BEM VII* (Edited by C. A. Brebbia and M. S. Ingber) pp. 589–604. CMP, Billerica, MA.

Bezine, G. P. (1978) Boundary integral formulation for plate flexure with arbitrary boundary conditions. *Mechanical Research Communications* **5**, 197–206.

Brebbia, C. A., Telles, J. C. F. and Wrobel, L. C. (1984) *Boundary Element Techniques: Theory and Applications in Engineering*. Springer, Berlin.

El-Zafrany, A., Debbih, M. and Fadhil, S. (1994) Boundary element analysis of thick Reissner plates in bending. *Engineering Analysis with Boundary Elements* **14**, 159–169.

El-Zafrany, A., Fadhil, S. and Debbih, M. (1995) An efficient approach for Boundary element bending analysis of thin and thick plates. *Computers and Structures* **56**, 565–576.

Guiggiani, M. (1996) Sensitivity analysis for boundary element error estimation and mesh refinement. *International Journal of Methods in Engineering* **39**, 2907–2920.

Guo-Shu, S. and Mukherjee, S. (1986) Boundary element method analysis of bending of elastic plates of arbitrary shape with general boundary conditions. *Engineering Analysis* **3**, 36–44.

Huber, O., Dallner, R., Partheymuller, P. and Kuhn, G. (1996) Evaluation of the stress tensor in 3-D elastoplasticity by direct solving of hypersingular integrals. *International Journal of Numerical Methods in Engineering* **39,** 2555–2573.
Karam, V. J. and Telles, J. C. F. (1988) On boundary elements for Reissner's plate theory. *Engineering Analysis* **5,** 21–27.
Karam, V. J. and Telles, J. C. F. (1992) The BEM applied to plate bending elastoplastic analysis using Reissner's theory. *Engineering Analysis with Boundary elements* **9,** 351–357.
Katsikadelis, J. T. and Yotis, A. J. (1993) A new boundary element solution of thick plates modelled by Reissner's theory. *Engineering Analysis with Boundary Elements* **12,** 65–74.
Long, S. Y., Brebbia, C. A. and Telles, J. C. F. (1988) Boundary element bending analysis of moderately thick plates. *Engineering Analysis* **5,** 64–74.
Paiva, J. B. (1991) Boundary element formulation for plate analysis with special distribution of reactions along the boundary. *Advances in Engineering Software* **13,** 162–168.
Paiva, J. B. and Neto, L. O. (1995) An alternative boundary element formulation for plate bending analysis. In *BETECH X* (Edited by M. H. Aliabadi and C. A Brebbia) pp. 1–8. CMP, Billerica, MA.
Paulino, G. H., Gray, L. J. and Zarikian, V. (1996) Hypersingular residuals : A new approach for error estimation in the boundary element method. *International Journal of Numerical Methods in Engineering* **39,** 2005–2029.
Portela, A., Aliabadi, M. H. and Rooke, D. P. (1993) Dual boundary element incremental analysis of crack propagation. *Computers and Structures* **46,** 237–247.
Reissner, E. (1945) The effect of transverse shear deformation on bending of elastic plates. *Journal of Applied Mathematics* **12,** A69–A77.
Reissner, E. (1947) On bending of elastic plates. *Quarterly Applied Mathematics* **5,** 55–68.
Stern, M. (1979) A general boundary integral formulation for the numerical solution of plates bending problems. *International Journal of Solids and Structures* **15,** 769–782.
Telles, J. C. F. (1987) A self-adaptive coordinate transformation for efficient numerical evaluation of general boundary element integrals. *International Journal of Numerical Methods in Engineering* **24,** 959–973.
Timoshenko, S. and Woinowsky-Krieger, S. (1959) *Theory of Plates and Shells*. McGraw-Hill, New York.
Timoshenko, S. and Goodier, J. N. (1934) *Theory of Elasticity*. McGraw-Hill, New York.
Tottenham, H. (1979) The boundary element method for plates and shells. In *Development in BEM*, (Edited by P. K. Banerjee & R. Butterfield), Vol. 1, pp. 173–205. Applied Science Publishers.
Vander Weeën, F. (1982a) Application of the boundary integral equation method to Reissner's plate model. *International Journal of Numerical Methods in Engineering* **18,** 1–10.
Vander Weeën, F. (1982b) Application of the direct boundary element method to Reissner's plate model. In *Boundary Element Methods in Engineering*, (Edited by C. A. Brebbia). Springer, Berlin.
Venturini, W. S. and Paiva, J. B. (1993) Boundary element for plate bending analysis. *Engineering Analysis with Boundary Elements* **11,** 1–8.
Westphal, T. Jr. and Barcellos, C. A. (1990) Application of the boundary element method to Reissner's and Mindlin's plate model. In *BEM XII* (Edited by M. Tanaka, C. A. Brebbia and T. Honna) Vol. 1, pp. 467–477. CMP, Billerica, MA.
Xiao-Yan, Lei (1995) A new BEM approach for Reissner's plate bending. *Computers and Structures* **54,** 1085–1090.

APPENDIX

The expression for the kernel U_{ij}^* are given by

$$U_{\alpha\beta}^* = \frac{1}{8\pi D(1-\nu)}\{[8B(z)-(1-\nu)(2\ln z-1)]\delta_{\alpha\beta}-[8A(z)+2(1-\nu)]r_{,\alpha}r_{,\beta}\}$$

$$U_{\alpha 3}^* = -U_{3\alpha}^* = \frac{1}{8\pi D}(2\ln z-1)rr_{,\alpha}$$

$$U_{33}^* = \frac{1}{8\pi D(1-\nu)\lambda^2}[(1-\nu)z^2(\ln z-1)-8\ln z] \tag{A1}$$

where

$$r^2 = (\mathbf{x}_\alpha-\mathbf{x}'_\alpha)(\mathbf{x}_\alpha-\mathbf{x}'_\alpha)$$

$$z = \lambda r$$

$$r_{,\alpha} = \frac{\partial r}{\partial \mathbf{x}_\alpha} \tag{A2}$$

The expression for the kernel P_{ij}^* are given by

$$P_{\gamma\alpha}^* = \frac{-1}{4\pi r}[(4A(z)+2zK_1(z)+1-\nu)(\delta_{\alpha\gamma}r_{,n}+r_{,\alpha}n_\gamma)$$
$$+(4A(z)+1+\nu)r_{,\gamma}n_\alpha-2(8A(z)+2zK_1(z)+1-\nu)r_{,\alpha}r_{,\gamma}r_{,n}]$$

$$p_{\gamma 3}^* = \frac{\lambda^2}{2\pi}[B(z)n_\gamma-A(z)r_{,\gamma}r_{,n}]$$

$$P^*_{3\alpha}=\frac{-(1-\nu)}{8\pi}\left[\left(2\frac{(1+\nu)}{(1-\nu)}\ln z-1\right)n_\alpha+2r_{,\alpha}r_{,\gamma}r_{,n}\right]$$

$$p^*_{33}=\frac{-1}{2\pi r}r_{,n} \tag{A3}$$

where $r_{,n}=r_{,\alpha}n_\alpha$.
The expression for the kernel $V^*_{i,\beta}$ are given by

$$V^*_{\alpha,\beta}=\frac{r^2}{128\pi D}[(4\ln z-5)\delta_{\alpha\beta}+2(4\ln z-3)r_{,\alpha}r_{,\beta}]$$

$$V^*_{3,\beta}=\frac{-rr_{,\beta}}{128\pi D(1-\nu)\lambda^2}[32(2\ln z-1)-z^2(1-\nu)(4\ln z-5)] \tag{A4}$$

The expression for the kernel U^*_{ijk} are given by

$$U^*_{\alpha\beta\gamma}=\frac{1}{4\pi r}[(4A(z)+2zK_1(z)+1-\nu)(\delta_{\beta\alpha}+\delta_{\alpha\gamma}r_{,\beta})$$
$$-2(8A(z)+2zK_1(z)+1-\nu)r_{,\alpha}r_{,\beta}r_{,\gamma}+(4A(z)+1+\nu)\delta_{\alpha\beta}r_{,\gamma}]$$

$$U^*_{\alpha\beta3}=\frac{-(1-\nu)}{8\pi}\left[\left(2\frac{(1+\nu)}{(1-\nu)}\ln z-1\right)\delta_{\alpha\beta}+2r_{,\alpha}r_{,\beta}\right]$$

$$U^*_{3\beta\gamma}=\frac{\lambda^2}{2\pi}[\beta(z)\delta_{\gamma\beta}-A(z)r_{,\gamma}r_{,\beta}]$$

$$U^*_{3\beta3}=\frac{1}{2\pi r}r_{,\beta} \tag{A5}$$

The expression for the kernel P^*_{ijk} are given by

$$P^*_{\alpha\beta\gamma}=\frac{D(1-\nu)}{4\pi r^2}\{(4A(z)+2zK_1(z)+1-\nu)(\delta_{\gamma\alpha}n_\beta+\delta_{\gamma\beta}n_\alpha)$$
$$+(4A(z)+1+3\nu)\delta_{\alpha\beta}n_\gamma-(16A(z)+6zK_1(z)+z^2K_0(z)+2-2\nu)$$
$$\times[(n_\alpha r_{,\beta}+n_\beta r_{,\alpha})r_{,\gamma}+(\delta_{\gamma\alpha}r_{,\beta}+\delta_{\gamma\beta}r_{,\alpha})r_{,n}]$$
$$-2(8A(z)+2zK_1(z)+1+\nu)(\delta_{\alpha\beta}r_{,\gamma}r_{,n}+n_\gamma r_{,\alpha}r_{,\beta})$$
$$+4(24A(z)+8zK_1(z)+z^2K_0(z)+2-2\nu)r_{,\alpha}r_{,\beta}r_{,\gamma}r_{,n}\}$$

$$P^*_{\alpha\beta3}=\frac{D(1-\nu)\lambda^2}{4\pi r}[(2A(z)+zK_1(z))(r_{,\beta}n_\alpha+r_{,\alpha}n_\beta)$$
$$-2(4A(z)+zK_1(z))r_{,\alpha}r_{,\beta}r_{,n}+2A(z)\delta_{\alpha\beta}r_{,n}]$$

$$P^*_{3\beta\gamma}=\frac{-D(1-\nu)\lambda^2}{4\pi r}[(2A(z)+zK_1(z))(\delta_{\gamma\beta}r_{,n}+r_{,\gamma}n_\beta)$$
$$+2A(z)n_\gamma r_{,\beta}-2(4A(z)+zK_1(z))r_{,\gamma}r_{,\beta}r_{,n}]$$

$$P^*_{3\beta3}=\frac{D(1-\nu)\lambda^2}{4\pi r^2}[(z^2B(z)+1)n_\beta-(z^2A(z)+2)r_{,\beta}r_{,n}] \tag{A6}$$

The expression for the kernel $W^*_{i\beta}$ are given by

$$W^*_{\alpha\beta}=\frac{-r}{64\pi}\{(4\ln z-3)[(1-\nu)(r_{,\beta}n_\alpha+r_{,\alpha}n_\beta)+(1+3\nu)\delta_{\alpha\beta}r_{,n}]$$
$$+4[(1-\nu)r_{,\alpha}r_{,\beta}+\nu\delta_{\alpha\beta}]r_{,n}\}-\frac{\nu}{(1-\nu)\lambda^2}U^*_{\alpha\beta\gamma}n_\gamma$$

$$W^*_{3\beta}=\frac{1}{8\pi}[(2\ln z-1)n_\beta+2r_{,\beta}r_{,n}]-\frac{\nu}{(1-\nu)\lambda^2}U^*_{3\beta\gamma}n_\gamma \tag{A7}$$